DOI 10.1007/s11182-024-03254-6
Russian Physics Journal, Vol. 67, No. 9, September, 2024

IMPACT TOUGHNESS OF HIGH-STRENGTH LOW-ALLOY STEELS JOINED BY FRICTION STIR WELDING

A. S. Dolzhenko, A. S. Lugovskaya, S. S. Malopheyev and A. N. Belyakov UDC 669.018.2

The microstructure and impact toughness of high-strength low-alloy steels joined by friction stir welding are studied. The hardened steel samples are tempered at a temperature of 600–650°C for 1 hour, followed by warm rolling to a total strain of 1.5 at the same temperature. The resulting steels are characterized by an ultrafine-grained lamella-type microstructure. The as-processed steel plates are joined by friction stir welding. A martensitic microstructure is formed in the stir zone. The steel samples with a carbon content of 0.15% show high impact toughness of 68 J/cm^2 at room temperature with a gradual decrease to 16 J/cm^2 at a temperature of –196°C, while the steel samples with a carbon content of 0.36% exhibit an impact toughness of 10 J/cm^2 at room temperature. The 0.36% carbon steel joints are tempered at a temperature of 650°C for 1 hour, which increases their room-temperature impact toughness to 67 J/cm^2.

Keywords: high-strength low-alloy steel, tempforming, friction stir welding, impact toughness, fractography.

INTRODUCTION

High-strength low-alloy steels are among the widely used classes of structural materials [1, 2]. One of their significant disadvantages is a relatively high temperature of the brittle-ductile transition, below which the impact toughness of these steels sharply drops; the steel becomes brittle, which can lead to a sudden catastrophic failure of the construction [3, 4]. In order to increase the impact toughness, these steels were subjected to tempforming. Tempforming was proposed by a group of Japanese scientists [5, 6] as a special thermo-mechanical treatment including rolling at a tempering temperature in order to provide a layered microstructure with a uniform distribution of the second phase particles and, therefore, to increase the impact toughness of carbon steels at low temperatures. Their studies [5, 6] have revealed that tempforming has a beneficial effect on the mechanical properties of high-strength low-alloy steels. In addition to improving impact toughness, tempforming strengthens the steels, increasing their yield strength. The high strength of tempformed steels is due to the small transverse grain size, the high dislocation density, and the finely dispersed carbides. Achieving such a unique combination of mechanical properties in high-strength low-alloy steels is of great practical importance. Such steels are promising materials for replacing the expensive maraging steels in the products manufactured in large series, intended for structures operating under shock loads at low temperatures.

High-strength low-alloy steels are also used to create lightweight welded constructions. Various technologies are used to connect parts made of high-strength steels, such as automatic welding, argon arc welding, and submerged arc welding. The main difficulty in welding high-strength low-alloy structural steels is their increased susceptibility to hardening, which leads to a sharp increase in the hardness of the metal in heat-affected zones (HAZs), which negatively affects the mechanical properties of welded joints. In addition, weld seams and HAZs of welded joints produced by traditional welding methods are characterized by a coarse-grained microstructure, which is an inevitable consequence of the welded steel melting. This is completely unacceptable for steels after tempforming, because their outstanding

Belgorod National Research University, Belgorod, Russia, e-mail: dolzhenko_a@bsu.edu.ru; malofeev@bsu.edu.ru; 1319927@bsu.edu.ru; belyakov@bsu.edu.ru. Original article submitted July 17, 2024, accepted for publication August 22, 2024.

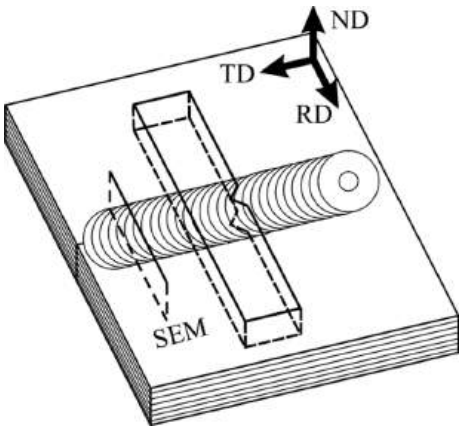

Fig. 1. Scheme of specimens preparation from friction stir welding joint.

mechanical properties are due to the formation of a specific microstructure with a transverse grain size much smaller than one micrometer. Unlike traditional welding methods, innovative friction stir welding (FSW), which is accompanied by large plastic deformation of the weld seam, makes it possible to form a weld joint with an ultra-fine-grained microstructure [7]. Recently, FSW has been applied to modern high-strength steels, including low-alloy steels subjected to tempforming [8–10]. Thus, the purpose of this work is to study the effect of FSW and additional tempering on the microstructure and impact toughness of the weld joints of high-strength low-alloy steels after tempforming.

MATERIAL AND METHODS

The present study was carried out on high-strength low-alloy Fe-0.15C-0.46Si-1.42Cr-1.32Mn-0.46Mo-0.17Ti and Fe-0.36C-0.4Si-0.56Cr-0.57Mn-0.54Mo (all in wt.%) steels, hereafter 0.15C and 0.35C steels, respectively. They were heated to 850°C, followed by water quenching. Tempforming was carried out as follows. The 0.15C and 0.35C steel billets were heated in a muffle furnace to tempering temperatures (600 and 650°C, respectively), maintained for an hour at these temperatures and then rolled in several passes to a total strain of 1.5. The rolling reduction per pass was 10%. After each pass, the steel blanks were reheated to tempering temperatures. The resulting 4 mm thick steel plates were joined by friction stir welding (FSW) using an AccuStir 1004 FSW machine to form a weld seam along the transverse direction (TD) as schematically shown in Fig. 1. The tool with a shoulder diameter of 11.26 mm and a hemispherical pin with a radius of 2.4 mm was made of tungsten carbide. The rotation speed of 400 rpm, the travel speed of 100 mm/min, the axial load of 4.5 kN, and the holding time of 3 s were used for 0.15C steel. The rotation speed of 400 rpm, the travel speed of 50 mm/min, the axial load of 4.4 kN, and the holding time of 3 s were used for 0.35C steel. After FSW, part of the 0.35C steel samples were tempered at 650°C for 1 hour.

The microstructures were examined using an FEI Quanta 600 scanning electron microscope equipped with an electron backscatter diffraction pattern (EBSP) analyzer using the TSL OIM Analysis 6 program. The orientation imaging microscopy (OIM) images were subjected to a cleanup procedure, i.e., the points with a confidence index of less than 0.1 were replaced by their neighbors. The average transverse grain and subgrain sizes were estimated on the OIM images as the average distances between the grain/subgrain boundaries with misorientations of $\theta \geq 15°$ and $\theta \geq 2°$, respectively, along the normal direction (ND).

The impact tests were carried out on the specimens with a cross-section of 2×8 mm^2 and a length of 55 mm with a V-shaped notch using an Instron 450 J impact machine with an Instron Dynatup Impulse data acquisition system in the temperature range from 20 to –196°C. The specimens for impact testing were cut so that the weld area was located in the middle of the specimen, i.e., in the notch area (Fig. 1). The fracture surfaces after impact tests were observed using a FEI Quanta 600 scanning electron microscope.

Fig. 2. Cross section of FSW joint of 0.15C steel.

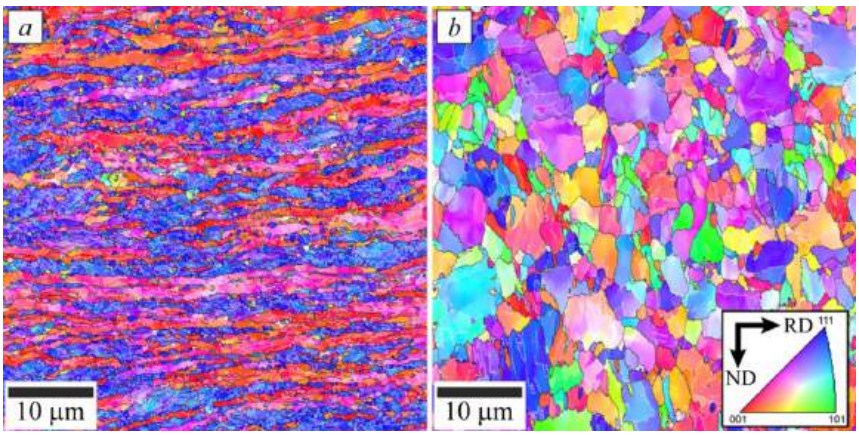

Fig. 3. Microstructures in base material (*a*) and stir zone (*b*) of 0.15C steel after FSW.

RESULTS AND DISCUSSION

1. Microstructure

Figure 2 shows a general view on the macrostructure of 0.15C steel in the cross section of the FSW joint (the macrostructure of 0.35C steel looks similar). The etching treatment clearly reveals both the upper and lower stir zones and the base material separated by semisphere-like borders. The microstructure in the upper stir zone looks like that of a martensite evolved during the second FSW pass. The lower part of the FSW seam developed during the first FSW pass and can, therefore, be considered as a tempered martensite. The microstructure in the zone close to the stir zone looks like a tempformed base material, although it has been affected by heating upon FSW. The base material can be characterized by a typical tempformed microstructure.

The base material microstructure and that formed in the stir zone of 0.15C steel after FSW is shown in Fig. 3. After tempforming, the base material microstructure consists of highly elongated grains with a transverse size of about 0.56 μm. This microstructure resulting from warm large-strain rolling (tempforming), is characterized by a two-component texture <111>//ND and <001>//ND (Fig. 2*a*), which is typical of warm-rolled carbon steels [11]. On the other hand, the microstructure formed in the stir zone consists of almost equiaxed grains, of an average size of 1.3 μm, with wavy boundaries (Fig. 2*b*). Different crystallographic orientations of the grains in Fig. 2*b* indicate a relatively weak texture in the stir zone.

The microstructures of 0.35C steel processed by tempforming at T_{TF} = 650°C and then subjected to FSW, as well as those after FSW and subsequent tempering at a temperature of 650°C, are shown in Fig. 4. After tempforming of 0.35C steel, a lamella-type microstructure consisting of elongated ultrafine grains with a transverse size of 0.36 μm and

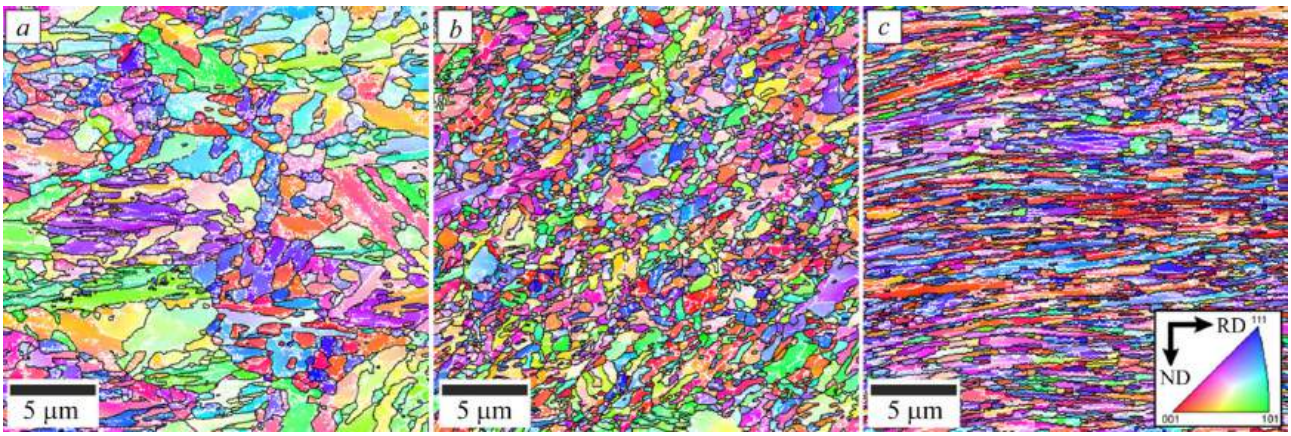

Fig. 4. Microstructures of 0.35 steel in stir zone after FSW (*a*), in stir zone after FSW and tempering at 650°C (*b*), and in base material after FSW and tempering at 650°C (*c*).

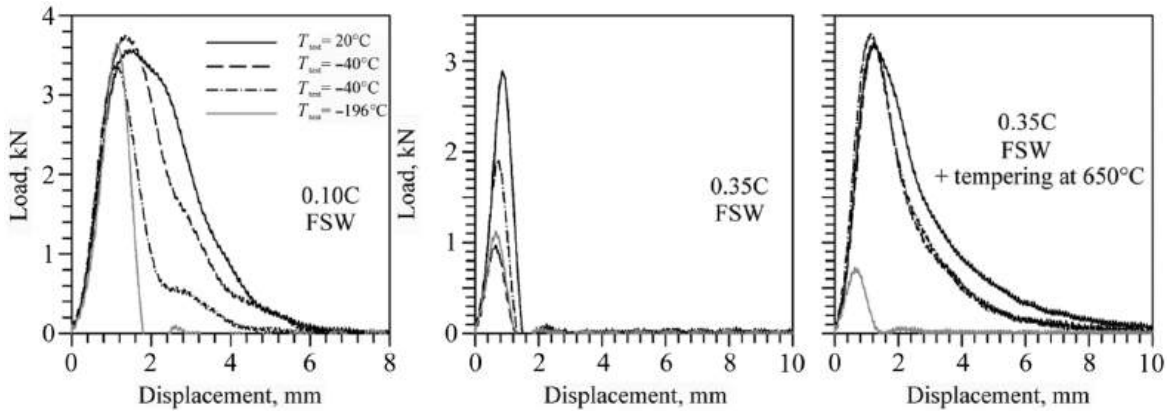

Fig. 5. Load-displacement curves of 0.15C and 0.35C steels subjected to FSW and impact tests at specified temperatures.

uniformly distributed dispersed carbide particles with an average size of 53 nm was formed in it. The stir zone is characterized by a lath martensitic microstructure consisting of ultrafine crystallites (Fig. 4*a*). The average grain size in the stir zone is 0.85 μm. It is obvious that the microstructure in the stir zone (Fig. 4*a*) has experienced the formation of secondary austenite followed by martensitic transformation during the FSW process. Subsequent tempering of this 0.35C steel at 650°C for 1 hour after FSW leads to the formation of a tempered martensite microstructure in the stir zone (Fig. 4*b*). After tempering, the average grain size does not significantly change and is about 0.85 μm. The base material subjected to FSW and post-weld tempering is characterized by a lamella-type microstructure (Fig. 4*c*) that is very similar to the initial tempformed microstructure. However, additional post-weld tempering at the tempforming temperature leads to an increase in the transverse grain size to 0.57 μm.

2. Impact toughness

The load-displacement curves constructed after impact testing of the high-strength low-alloy steels are presented in Fig. 5. A sample of 0.15C steel after FSW, tested at room temperature, demonstrates high adsorbed impact energy. The total fracture energy is mainly spent on the initiation of critical-size cracks and on the stable crack

TABLE 1. Impact Toughness of Experimental Steel Samples

Sample	KCV, J/cm^2			
	T = 20°C	T = –40°C	T = –60°C	T = –196°C
0.15C, FSW	68	59	37	16
0.35C, FSW	10	2	5	2.5
0.35C, FSW + tempering at 650°C	67	49	52	1.2

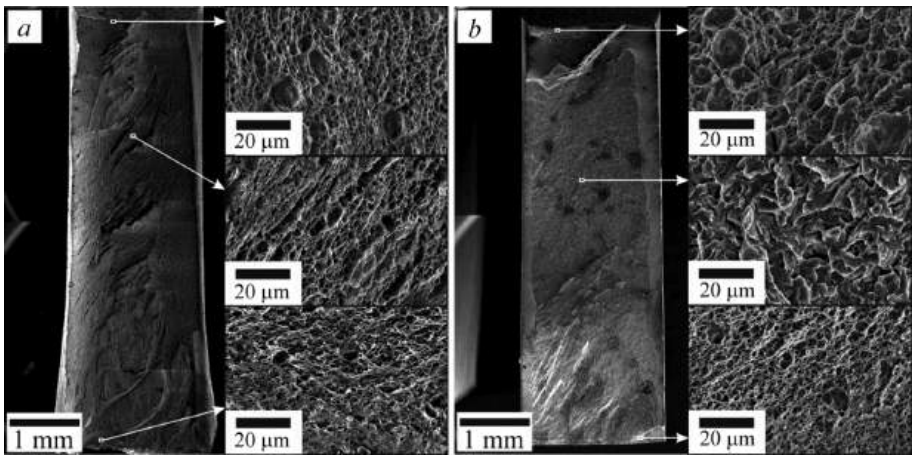

Fig. 6. Fracture surfaces of 0.15C steel subjected to FSW and impact tests at 20°C (*a*) or –196°C (*b*).

propagation. A decrease in the test temperature reduces the impact toughness and shortens the stable crack propagation stage. At test temperatures below –60°C, the onset of unstable crack propagation occurs almost immediately after the maximum load. At all test temperatures, the maximum load is in the range from 3.3 to 3.8 kN. The impact toughness decreases from 68 to 16 J/cm^2 with a decrease in the test temperature from 20°C to –196°C (Table 1).

The 0.35C steel sample after FSW demonstrates low values of impact toughness throughout the entire temperature range under study. None of the curves contain a stage of stable crack propagation. As the test temperature decreases from room temperature to –60°C, the maximum load decreases by 3 times. Tempering of 0.35C steel after FSW leads to a significant increase in the impact toughness to 67 and 52 J/cm^2 at room temperature and at –60°C, respectively. The maximum load values during impact tests in the temperature range from 20 to –60°C increase to 3.3 kN. As the test temperature decreases to the liquid nitrogen temperature, the maximum load decreases by nearly 5 factors.

The data on the static strength properties of the FSW joints of these steels are presented elsewhere [12, 13].

3. Fractography

The fracture surface images of FSW 0.15C steel samples after impact tests are presented in Fig. 6. A ductile fracture character is observed after impact bending test at room temperature (Fig. 6*a*). The fracture surface consists of crack initiation, stable crack propagation, and failure zones [14–18]. In all zones, a dimple fracture surface is observed, resulting from the micropore coalescence. The shapes of the dimples in the fracture zones differ. In the nucleation zone, small dimples predominate, alternating with rather large ones. On the other hand, there is a uniform distribution of elongated pits in the failure zone. Individual particles located at the bottom of the dimples suggest the nucleation of micropores on them [19]. Stable crack propagation occurs through a ductile mechanism with the formation of dimples. After testing at liquid nitrogen temperature, the crack initiation and failure zones become smaller in comparison with the fracture surface after testing at room temperature characterized by ductile dimple fracture (Fig. 6*b*). In the zone of

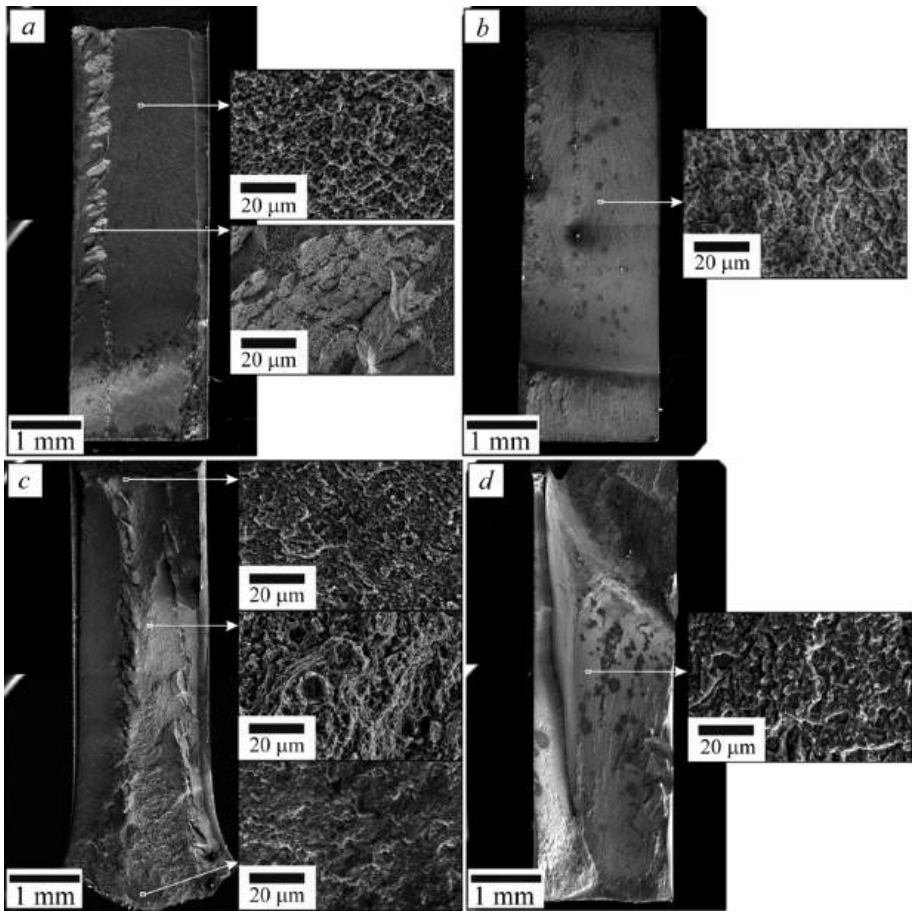

Fig. 7. Fracture surfaces of 0.35C steel subjected to FSW and impact tests at 20°C (*a*) or –196°C (*b*); fracture surfaces of 0.35C steel subjected to FSW followed by tempering at 650°C and impact tests at 20°C (*c*) or –196°C (*d*).

unstable crack propagation, quasi-cleavage transgranular fracture is observed, which is characterized by the presence of cleavage facets on the fracture surface.

The images of the fracture surfaces of FSW 0.35C steel samples after impact tests are shown in Fig. 7*a*, *b*. Over the entire test temperature range, the fracture is brittle. The onset of unstable crack propagation occurs immediately after the pendulum contacts the sample. There are cleavage facets observed on all fracture surfaces.

The images of the fracture surfaces of 0.35C steel subjected to FSW followed by tempering at 650°C and impact tests are presented in Fig. 7*c*, *d*. Ductile fracture is observed after impact bending test at room temperature (Fig. 7*c*). The fracture surface consists of a crack initiation zone, a stable crack propagation zone, and a failure zone. All zones are characterized by ductile fracture, as evidenced by the presence of dimples that differ only in shape and size. After testing at liquid nitrogen temperature, the sample surface represents a zone of unstable crack propagation containing cleavage facets, which indicates brittle fracture.

CONCLUSIONS

The microstructure and impact toughness of high-strength low-alloy steels subjected to tempforming and friction stir welding (FSW) have been studied. The results can be summarized as follows.

1. FSW of the 0.15C steel samples after tempforming leads to the formation of austenite followed by martensitic transformation upon cooling in the stir zone of the weld. The initial layered microstructure with a transverse grain size of 0.56 μm after tempforming is replaced by a fine-grained structure with an average grain size of 1.3 μm in the stir zone. The stir zone of the tempformed 0.35C steel sample after FSW is characterized by a lath martensite microstructure with an average grain size of 0.85 μm, due to heating to the austenitic temperature and rapid cooling after FSW.

2. The impact toughness of the 0.15C steel samples after FSW decreases from 68 to 16 J/cm^2 with a decrease in the test temperature from 20 to –196°C. In contrast, the 0.35C steel samples after FSW show low values of impact toughness of 10 J/cm^2 even at room temperature. An additional tempering after FSW increases the impact toughness of the 0.35C steel to 67 J/cm^2 at room temperature and to 52 J/cm^2 at –60°C.

3. FSW joints of the steel with a carbon content of about 0.15% have an impact strength of more than 50 J/cm^2 at –40°C. Increasing the carbon content in steel to 0.35% leads to a decrease in the impact toughness of the FSW joints to 10 J/cm^2 at room temperature. An additional tempering of joints of such FSW steel joints allows increasing the impact toughness to 50 J/cm^2 at room and lowered temperatures.

COMPLIANCE WITH ETHICAL STANDARDS

Funding and acknowledgement

The present work was carried out under a grant of the Russian Science Foundation (No. 20-19-00497-П) using the equipment of the Technologies and Materials Joint Research Center of the Belgorod National Research University.

REFERENCES

1. F. Goodwin, S. Guruswamy, K. U. Kainer, C. Kammer, W. Knabl, G. Leichtfried, G. Schlamp, R. Stickler and H. Warlimont, Metals, in: Springer Handbook of Condensed Matter and Materials Data (Eds. W. Martienssen and H. Warlimont), Springer, Berlin (2005).
2. G. Krauss, Steels – Processing Structure and Performance, ASM International, Phoenix (2015). http://doi.org/10.31399/asm.tb.spsp2.9781627082655.
3. B. Faucher and B. Dogan, Metall. Trans. A, **19,** 505 (1988). http://doi.org/10.1007/BF02649265.
4. Y. Tomita, Mater. Sci. Technol., **4,** 613 (1988). https://doi.org/10.1179/mst.1988.4.7.613
5. Y. Kimura, T. Inoue, F. Yin, O. Sitdikov and K. Tsuzaki, Scripta Mater., **57,** No. 6, 465 (2007). http://doi.org/10.1016/j.scriptamat.2007.05.039.
6. T. Inoue, H. Qiu, R. Ueji and Y. Kimura, Mater., **14,** 1634 (2021). http://doi.org/10.3390/ma14071634.
7. R. Al-Sabur, Mater. Today Proc., **45,** 4504 (2021). https://doi.org/10.1016/j.matpr.2020.12.1001.
8. M. Santella, Y. Hovanski and T.-Y. Pan, SAE Int. J. Mater. Manuf., **5,** 382 (2012). https://doi.org/10.4271/2012-01-0480.
9. H. Lee, C. Kim and J.H. Song, Mater., **8,** 8424 (2015). https://doi.org/10.3390/ma8125467.
10. V. Abhilash and A.K. Lakshminarayanan, Mater. Res. Express, **10,** 026505 (2023). https://doi.org/10.1088/2053-1591/acb63e.
11. L. A. I. Kestens and H. Pirgazi, Mater. Sci. Technol., **32**, 1303 (2016). https://doi.org/10.1080/02670836.2016.1231746.
12. A. Dolzhenko, S. Malopheyev, A. Lugovskaya, V. Dudko, M. Tikhonova, R. Kaibyshev and A. Belyakov. Steel Res. Int., **95**(5) 2300812 (2024). https://doi.org/10.1002/srin.202300812.
13. A. Dolzhenko, A. Lugovskaya, S. Malopheyev, V. Dudko, M. Tikhonova, R. Kaibyshev and A. Belyakov.. Metals, **14**(1) 114 (2024). https://doi.org/10.3390/met14010114.
14. ASM Handbook. Volume 8: Mechanical Testing and Evaluation (Eds. H. Kuhn and D. Medlin), ASM International, Materials Park (2000). https://doi.org/10.31399/asm.hb.v08.9781627081764.

15. A. Chatterjee, D. Chakrabarti, A. Moitra, R. Mitra and A. Bhaduri, Mater. Sci. Eng. A, **630,** 58 (2015). https://doi.org/10.1016/j.msea.2015.01.076.
16. V. Dudko, A. Fedoseeva and R. Kaibyshev, Mater. Sci. Eng. A, **682,** 73 (2017). https://doi.org/10.1016/j.msea.2016.11.035.
17. N. Dudova, R. Mishnev and R. Kaibyshev, ISIJ Int. **51,** 1912 (2011). https://doi.org/10.2355/isijinternational.51.1912.
18. R. Chaouadi and A. Fabry, Eur. Struct. Integr. Soc., **30,** 103 (2002). https://doi.org/10.1016/S1566-1369(02)80011-5.
19. ASM Metals Handbook, Fractography, ASM International (1987).